Five-Coordinate $[RuCl(P-P^*)_2]^+$ Complexes Containing Chiral Diphosphines: Application in the Asymmetric Cyclopropanation and Epoxidation of Olefins

Robert M. Stoop, Christian Bauer, Patrick Setz, Michael Wörle, Terrance Y. H. Wong, and Antonio Mezzetti*

Laboratorium für Anorganische Chemie, ETH-Zentrum, CH-8092 Zürich, Switzerland

Received August 16, 1999

The six-coordinate complexes *trans*-$[RuCl_2(P-P^*)_2]$ (P−P* = (*S*,*S*)-1,2-bis(1-naphthylphenylphosphino)ethane (bnpe), **2a**; (*S*,*S*)-2,3-bis(diphenylphosphino)butane (chiraphos), **2b**) have been prepared and structurally characterized. The X-ray studies of **2a**,**b** show non-C_2-symmetric conformations of the substituents at the PPh_2 groups in a highly crowded octahedral environment. Complexes **2a**,**b** react with $Tl[PF_6]$ in CH_2Cl_2 to give the corresponding monochloro, cationic derivatives $[RuCl(P-P^*)_2]PF_6$ (P−P* = bnpe, **3a**; chiraphos, **3b**). The bnpe derivative **3a** is five-coordinate both in the solid state (by X-ray investigation) and in solution (by ^{31}P NMR spectroscopy). The chiraphos analogue **3b** apparently dimerizes in solution, depending on the solvent ($CDCl_3$ or CD_2Cl_2) and on the concentration. Complexes **3a**,**b** catalyze the decomposition of ethyl diazoacetate to give, in the presence of styrene, the corresponding cyclopropanation products with enantioselectivity up to 35% ee and *E*/*Z* ratios of about 55:45. Complexes **3a**,**b** also catalyze the epoxidation of unfunctionalized olefins with iodosyl benzene as the primary oxidant. High olefin conversions and fair selectivity for the epoxide are observed, but both **3a** and **3b** give racemic epoxide.

Introduction

In the reactions catalyzed by transition metal complexes, coordinative unsaturation at the metal is generally considered as condition *sine qua non* for catalytic activity. This is a particular issue with the iron group metals, where six-coordination is the norm. However, unsaturation can play different roles, depending on the catalytic system. Thus, in homogeneous hydrogenation the unsaturated metal center activates the dihydrogen molecule, either homolytically or heterolytically, and often also the olefin.[1] In other catalytic reactions, such as cyclopropanation[2] and epoxidation,[3] the role of the metal is rather to stabilize a reactive fragment X (a carbene or oxo ligand) in a coordinatively saturated complex of the type $[M(CR_2)L_5]$ or $[M(O)L_5]$. The fragment X (= CHR or O) is generally believed to be transferred to the *uncoordinated* olefin substrate.[2,3] This poses a problem in asymmetric catalysis, as the interactions involved in enantioface discrimination are weaker than when substrate precoordination leads to diastereomeric complexes.[3a,b]

To improve the enantioselectivity, tetradentate ligands have been used in epoxidation and cyclopropanation reactions catalyzed by the iron group metals, in particular porphyrins,[4] Schiff bases,[5] oxazoline derivatives,[6] or hybrid ligands containing imino and phosphino functionalities.[7] Thus, we have recently shown that ruthenium(II) complexes containing the hybrid phosphino imino ligand (*S*,*S*)-bis(*o*-diphenylphosphinobenzylidene)diimminocyclohexane efficiently catalyze the epoxidation of unfunctionalized olefins with hydrogen peroxide as the primary oxidant.[7a]

Lately, chiral tridentate ligands have found successful application in asymmetric cyclopropanation[8] and epoxi-

* To whom correspondence should be addressed. Fax: ++41 1 632 13 10. E-mail: mezzetti@inorg.chem.ethz.ch.

(1) For a review, see: Chaloner, P. A.; Esteruelas, M. A.; Joó, F.; Oro, L. A. *Homogeneous Hydrogenation*; Kluwer: Dordrecht, 1994; Chapter 1.

(2) See, for instance: (a) Cornils, B.; Herrmann, W. A. *Applied Homogeous Catalysis with Organometallic Compounds*, 1st ed.; VCH: New York, 1996; Vols. 1−2. (b) Doyle, M. P.; McKervey, A. M.; Ye, T. *Modern Catalytic Methods for Organic Synthesis with Diazocompounds, from Cyclopropanes to Ylides*, 1st ed.; Wiley: New York, 1998.

(3) See, for instance: (a) Jacobsen, E. N. In *Catalytic Asymmetric Synthesis*; Ojima, I, Ed.; VCH Publishers: New York, 1993; Chaper 4.2. (b) Ito, Y. N.; Katsuki, T. *Bull. Chem. Soc. Jpn.* **1999**, *72*, 603. (c) Nugent, W. A.; Mayer, J. M. *Metal−Ligand Multiple Bonds*; Wiley: New York, 1988. (d) Lin, Z.; Hall, M. B. *Coord. Chem. Rev.* **1993**, *123*, 149. (e) Drago, R. S. *Coord. Chem. Rev.* **1992**, *117*, 185. (f) Jørgensen, K. A. *Chem. Rev.* **1989**, *89*, 431.

(4) Recent papers: (a) Gross, Z.; Ini, S. *Inorg. Chem.* **1999**, *38*, 1446. (b) Lai, T. S.; Kwong, H. L.; Zhang, R.; Che, C. M. *J. Chem. Soc., Dalton Trans.* **1998**, 3559. (c) Berkessel A.; Frauenkron, M. *J. Chem. Soc., Perkin Trans.* **1997**, 2265. (d) Galardon, E.; Roue, S.; Le Maux, P.; Simonneaux, G. *Tetrahedron Lett.* **1998**, *36*, 2333. (e) Berkessel, A.; Frauenkron, M. *Tetrahedron Lett.* **1997**, *38*, 7175. (f) Lo, W. C.; Cheng, K. F.; Che, C. M.; Mak, T. C. W. *Chem. Commun.* **1997**, 1205.

(5) Recent papers: (a) Cheng, M. C.; Chan, M. C. W.; Peng, S. M.; Cheung, K. K.; Che, C. M. *J. Chem. Soc., Dalton Trans.* **1997**, 3479. (b) Kureshi, R. I.; Khan, N. H.; Abdi, S. H. R.; Iyer, P. *J. Mol. Catal. A-Chem.* **1997**, *124*, 91. (c) Bernardo, K.; Leppard, S.; Robert, A.; Commenges, G.; Dahan, F.; Meunier, B. *Inorg. Chem.* **1996**, *35*, 387.

(6) See, for instance: (a) End, N.; Pfaltz, A. *Chem. Commun.* **1998**, 589. (b) Mizushima, K.; Nakaura, M.; Park, S. B.; Nishiyama, H.; Monjushiro, H.; Harada, K.; Haga, M. *Inorg. Chim. Acta* **1997**, *261*, 175.

(7) Recent papers: (a) Stoop, R. M.; Mezzetti, A. *Green Chem.* **1999**, 39. (b) Song, J.-H.; Cho, D.-J.; Jeon, S.-J.; Kim, Y.-H.; Kim, T.-J.; Jeong, J. H. *Inorg. Chem.* **1999**, *38*, 893.

(8) Recent papers: (a) Lee, H. M.; Bianchini, C.; Jia, G. C.; Barbaro, P. *Organometallics* **1999**, *18*, 1961. (b) Barbaro, P.; Bianchini, C.; Togni, A. *Organometallics* **1997**, *16*, 3004. (c) Nishiyama, H.; Soeda, N.; Naito, T.; Motoyama, Y. *Tetrahedron: Asymmetry* **1998**, *9*, 2865.

10.1021/om990657x CCC: $18.00
Publication on Web 12/02/1999

Chart 1

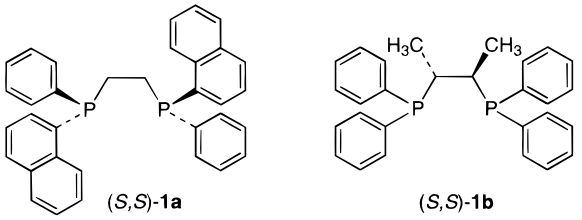

dation[9] catalyzed by ruthenium complexes. By contrast, bidentate ligands have been rarely used in these reactions,[10] and reports involving diphosphino complexes are rare and restricted to achiral ligands.[11] Moreover, we are not aware of any catalytic transformations that use ruthenium complexes of chiral diphosphines of the type $[RuCl(P-P^*)_2]^+$. This may sound surprising in view of the large number of chiral diphosphine ligands now available, but can be probably explained by the fact that non-hydride ruthenium(II) complexes are difficult to prepare when the diphosphine is very bulky.

We have undertaken the study of five-coordinate, cationic complexes of the type $[RuCl(P-P^*)_2]^+$ (P−P* = chiral diphosphine) as catalysts for the enantioselective epoxidation and cyclopropanation of olefins. As these complexes are the chiral *pendant* of $[RuCl(dppp)_2]^+$,[12] which has been previously used as epoxidation catalyst,[11] we started our investigation with the enantioselective epoxidation and cyclopropanation of olefins. In particular, the cationic complexes $[RuCl(P-P)_2]^+$ are expected to be more active catalysts than the neutral species $[RuCl_2L_3]$ (L = phosphine).[8a,b] We report here the synthesis and X-ray structures of [RuCl((*S,S*)-bnpe)]$^+$ (bnpe = 1,2-bis(1-naphthylphenylphosphino)-ethane) and [RuCl((*S,S*)-chiraphos)]$^+$ (chiraphos = 2,3-bis(diphenylphosphino)butane), together with the first catalytic results.

Results and Discussion

Diphosphine Ligands. The ligands 1,2-bis(1-naphthylphenylphosphino)ethane (bnpe, **1a**) and 2,3-bis-(diphenylphosphino)butane (chiraphos, **1b**) (Chart 1) were chosen for this study, after chiral ligands forming six- or seven-membered chelate rings failed to form complexes of the type $[RuCl_2(P-P^*)_2]$ or $[RuCl(P-P^*)_2]^+$ from a variety of dichloro-containing precursors. In fact, binap,[13a] biphemp,[13b] Josiphos,[13c] and *C,C′*-tetramethylsilanebis(1-naphthylphenylphosphine)[13d] react with $[RuCl_2(PPh_3)_3]$ to give monosubstituted products of the type $[RuCl_2(PPh_3)(P-P^*)]$ or $[RuCl_2(P-P)]_2$.[13d,e] This is probably due to the combined effects of increased steric bulk of the diphosphine and reduced trans effect of chloride as compared to hydride, as the corresponding analogues $[RuH(P-P)_2]^+$ can be prepared with a general procedure.[14]

Scheme 1

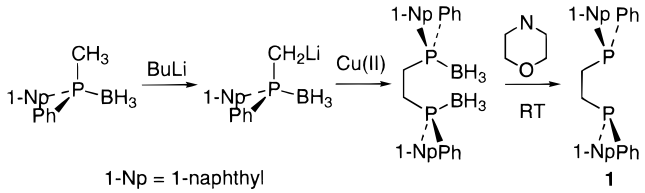

Enantiomerically pure 1,2-bis(1-naphthylphenylphosphino)ethane (bnpe, **1a**) is prepared by deprotonation and oxidative coupling of the phosphine borane (*S*)-P(BH$_3$)(Me)(Ph)(1-Np) (Scheme 1). The latter is obtained by the procedure published previously,[13d] which follows the general method developed by Jugé.[15] Deboranation of the BH$_3$-protected diphosphine **1a**·(BH$_3$)$_2$ gives enantiomerically pure (*S,S*)-bnpe (**1a**). This is shown by reprotection of **1a** with BH$_3$·SMe$_2$ and chiral HPLC analysis of **1a**·(BH$_3$)$_2$, by comparison with the diastereomeric mixture (*l*)+(*u*)-**1a**·(BH$_3$)$_2$ (see Experimental Section). This is the first stereoselective synthesis of bnpe. To the best of our knowledge, there is a single report dealing with bnpe, in which enantiomerically pure $[Rh(COD)(bnpe)]^+$ (COD = 1,5-cyclooctadiene) has been prepared by racemic resolution of the diastereomeric camphorsulfonate (Y^-) salts [Rh(COD)((*l*)-bnpe)]Y.[16]

[RuCl$_2$(P−P*)$_2$]. The complexes $[RuCl_2(P-P^*)_2]$ (P−P* = bnpe, **2a**; chiraphos, **2b**) are prepared from $[RuCl_2(PPh_3)_3]$ by ligand exchange in CH_2Cl_2 at room temperature.[17] In both cases, only the trans isomer is formed, as indicated by the singlet in the ^{31}P NMR spectrum. The X-ray structure of both complexes was determined. The crystals of **2a** contain discrete $[RuCl_2(bnpe)_2]$ units with the metal in a severely distorted octahedral environment featuring trans chloro ligands (Figure 1). The complex is nearly C_2-symmetric, with the pseudobinary axis bisecting the P(1)−Ru−P(4) angle. The two P atoms of each bnpe, e.g., P(1) and P(2), are inequivalent (see below). The overall geometry is determined by the steric crowding due to the large naphthyl groups. Although the four P atoms are fairly coplanar within ±0.07 Å, the Cl(1)−Ru−Cl(2) angle is closed down to 166.68(5)° due to the short nonbonded contacts between the Cl atoms and the naphthyl groups on P(1) and P(4) (Table 1). Accordingly, the Cl−Ru−P angles show that the naphthyl groups on P(1) and P(4) push the Cl atoms toward P(3) and P(2), respectively. The Ru−Cl and Ru−P distances (average 2.453(1) and 2.410(1) Å, respectively) fall in the upper quartile of the range

(9) See, for instance: (a) Nishiyama, H.; Shimada, T.; Ito, H.; Sugiyama, H.; Motoyama, Y. *Chem. Commun.* **1997**, 1863. (b) Cetinkaya, B.; Cetinkaya, E.; Brookhart, M.; White, P. S. *J. Mol. Catal. A-Chem.* **1999**, *142*, 101.

(10) Recent papers: (a) Barf, G. A.; van den Hoek, D.; Sheldon, R. A. *Tetrahedron* **1996**, *52*, 12971. (b) Boelrijk, A. E. M.; Neenan, T. X.; Reedijk, J. *J. Chem. Soc., Dalton Trans.* **1997**, 4561. (c) Augier, C.; Malara. L.; Lazzeri, V.; Waegell, B. *Tetrahedron Lett.* **1995**, *36*, 8775.

(11) (a) Bressan, M.; Morvillo, A. *Inorg. Chem.* **1989**, *28*, 950. (b) Morvillo, A.; Bressan, M. *J. Mol. Catal. A-Chem.* **1997**, *125*, 119. (c) Maran, F.; Morvillo, A.; d'Alessandro, N.; Bressan, M. *Inorg. Chim. Acta* **1999**, *288*, 122.

(12) Bressan, M.; Rigo, P. *Inorg. Chem.* **1975**, *14*, 2286.

(13) (a) Noyori, R.; Takaya, H. *Acc. Chem. Res.* **1990**, *23*, 345. (b) Schmid, R.; Cereghetti, M.; Heiser, B.; Schönholzer, P.; Hansen, H.-J. *Helv. Chim. Acta* **1988**, *71*, 897. (c) Togni, A.; Breutel, C.; Schnyder, A.; Spindler, F.; Landert, H.; Tijani, A. *J. Am. Chem. Soc.* **1994**, *116*, 4062. (d) Stoop, R. M.; Mezzetti, A.; Spindler, F. *Organometallics* **1998**, *17*, 668. (e) Mezzetti, A.; Tschumper, A.; Consiglio, G. *J. Chem. Soc., Dalton Trans.* **1995**, 49.

(14) See for instance: Ogasawara, M.; Saburi, M. *Organometallics* **1994**, *13*, 1911.

(15) Jugé, S.; Stéphan, M.; Laffitte, J. A.; Genet, J. P. *Tetrahedron Lett.* **1990**, *31*, 6357.

(16) Yoshikuni, T.; Bailar, J. C. *Inorg. Chem.* **1982**, *21*, 2129.

(17) [RuCl$_2$(chiraphos)$_2$] has been briefly reported previously: (a) Ikariya, T.; Ishii, Y.; Kawano, H.; Arai, T.; Saburi, M.; Yoshikawa, S.; Akutagawa, S. *J. Chem. Soc., Chem. Commun.* **1985**, 922. (b) James, B. R.; Fogg, D. E. *J. Organomet. Chem.* **1993**, *462*, C21.

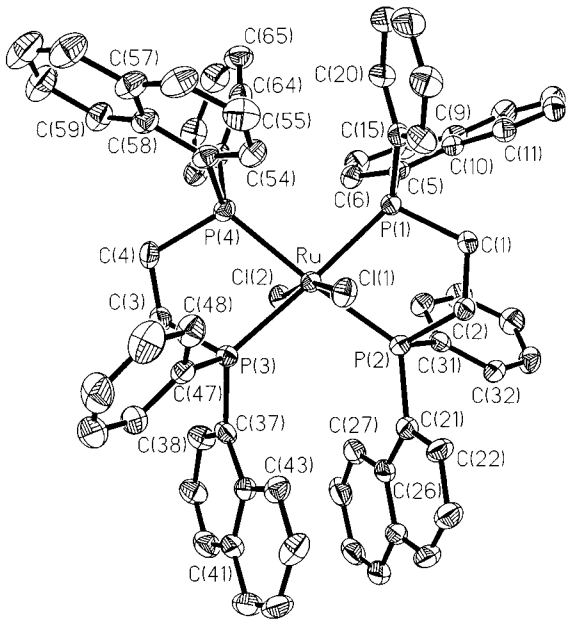

Figure 1. ORTEP view of [$RuCl_2$(bnpe)$_2$], **2a**.

Table 1. Selected Interatomic Distances (Å) and Angles (deg) in [$RuCl_2$(bnpe)$_2$] (2a)

Ru−Cl(1)	2.449(1)	Ru−Cl(2)	2.457(1)
Ru−P(1)	2.415(1)	Ru−P(2)	2.412(1)
Ru−P(3)	2.409(1)	Ru−P(4)	2.406(1)
Cl(1)···C(16)	3.486(7)	Cl(2)···C(6)	3.225(6)
Cl(1)···C(48)	3.222(7)	Cl(2)···C(36)	3.348(7)
Cl(1)···C(54)	3.373(6)	Cl(2)···C(63)	3.401(6)
Cl(1)−Ru−Cl(2)	166.68(5)		
Cl(1)−Ru−P(1)	87.51(5)	Cl(1)−Ru−P(2)	83.71(5)
Cl(1)−Ru−P(3)	90.44(5)	Cl(1)−Ru−P(4)	99.94(5)
Cl(2)−Ru−P(1)	102.04(5)	Cl(2)−Ru−P(2)	88.98(5)
Cl(2)−Ru−P(3)	80.46(5)	Cl(2)−Ru−P(4)	88.32(5)
P(1)−Ru−P(2)	78.98(5)	P(1)−Ru−P(3)	176.47(5)
P(1)−Ru−P(4)	96.45(5)	P(2)−Ru−P(3)	103.67(5)
P(2)−Ru−P(4)	174.08(5)	P(3)−Ru−P(4)	81.07(5)

observed for ruthenium complexes,[18] which is a further indication of steric crowding.

Both chelate rings adopt an envelope conformation with the two flaps, P(2) and P(3), lying above and below the RuP_4 plane. In the first one, Ru, P(1), C(1), and C(2) are coplanar within ±0.05 Å, and P(2) is displaced from their mean plane by 1.00 Å (Figure 2). In the second one, Ru, P(4), C(3), and C(4) are coplanar within ±0.12 Å, and P(3) is displaced by 0.87 Å. As a consequence, the naphthyl and phenyl groups on P(2) and P(3) occupy the equatorial and axial positions, respectively. The flattening at P(1) and P(4) makes the equatorial and axial positions nearly equivalent: Figure 2 shows that the orientation of the 1-naphthyl and phenyl substituents on P(1) is nearly the same, although their steric requirements largely differ. Eventually, the substituents at the P atoms of each bnpe ligand assume a *syn*-diaxial,*syn*-diequatorial conformation. Similar conformations are found in *trans*-[$RuCl_2$($Ph_2PCH_2CH_2PPh_2$)$_2$][19] and in *trans*-[$RuCl_2$(chiraphos)$_2$] (see below), whereas in *trans*-[$RuCl_2$((*S,S*)-$MePhPCH_2CH_2PMePh$)$_2$] both chelate rings assume a half-chair conformation with the phenyls in the less hindered equatorial positions.[20]

(18) Orpen, A. G.; Brammer, L.; Allen, F. H.; Kennard, O.; Watson, D. G.; Taylor, R. *J. Chem. Soc., Dalton Trans.* **1989**, S1.
(19) Polam, J. R.; Porter, L. C. *J. Coord. Chem.* **1993**, *29*, 109.
(20) Wartchow, R.; Berthold, H. J *Z. Kristallogr.* **1977**, *145*, 240.

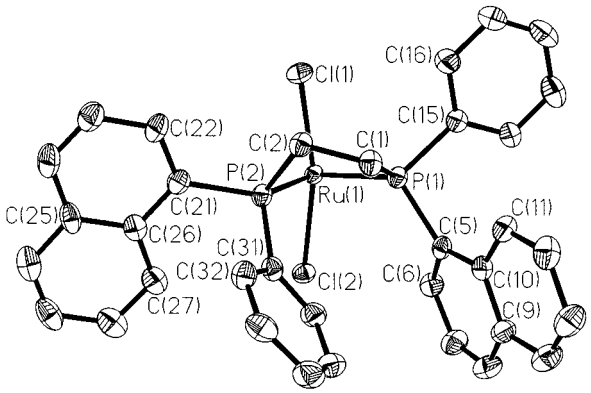

Figure 2. ORTEP view of [$RuCl_2$(bnpe)$_2$] (**2a**) along the RuP_4 plane. The second bnpe ligand is omitted for clarity.

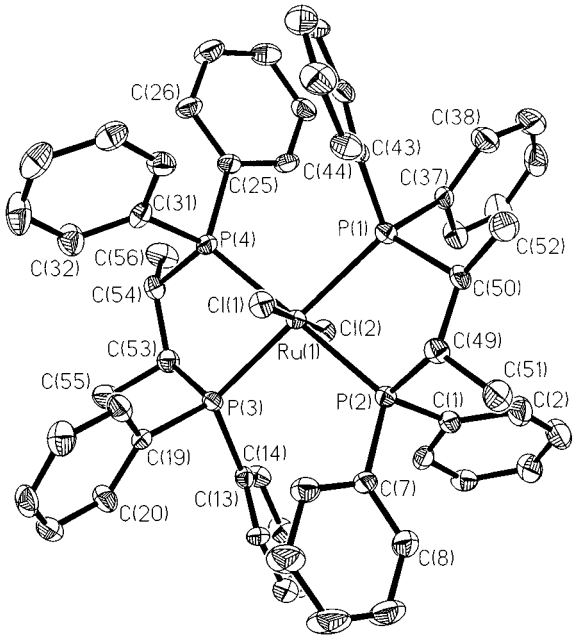

Figure 3. ORTEP view of [$RuCl_2$(chiraphos)$_2$], **2b**.

Table 2. Selected Interatomic Distances (Å) and Angles (deg) in [$RuCl_2$(chiraphos)$_2$] (2b)

Ru(1)−Cl(1)	2.435(2)	Ru(1)−Cl(2)	2.451(2)
Ru(1)−P(1)	2.431(2)	Ru(1)−P(2)	2.368(2)
Ru(1)−P(3)	2.385(2)	Ru(1)−P(4)	2.367(2)
Cl(1)···C(12)	3.454(7)	Cl(2)···C(30)	3.523(7)
Cl(1)···C(24)	3.299(7)	Cl(2)···C(42)	3.326(7)
Cl(1)−Ru(1)−Cl(2)	178.75(6)		
Cl(1)−Ru(1)−P(1)	82.95(7)	Cl(1)−Ru(1)−P(2)	86.45(6)
Cl(1)−Ru(1)−P(3)	99.36(7)	Cl(1)−Ru(1)−P(4)	90.34(7)
Cl(2)−Ru(1)−P(1)	97.33(7)	Cl(2)−Ru(1)−P(2)	94.80(6)
Cl(2)−Ru(1)−P(3)	80.37(7)	Cl(2)−Ru(1)−P(4)	88.41(6)
P(1)−Ru(1)−P(2)	81.00(6)	P(1)−Ru(1)−P(3)	177.68(8)
P(1)−Ru(1)−P(4)	99.25(6)	P(2)−Ru(1)−P(3)	98.86(6)
P(2)−Ru(1)−P(4)	176.73(7)	P(3)−Ru(1)−P(4)	81.03(6)

The crystal of the chiraphos derivative *trans*-[$RuCl_2$-(chiraphos)$_2$] (**2b**) contains two independent molecules in the unit cell, with approximately the same distorted octahedral coordination. As most structural parameters of the two molecules are very similar, only one is described below. As in **2a**, a pseudo-C_2 axis bisects the P(1)−Ru−P(4) angle (Figure 3). Although the Cl(1)−Ru−Cl(2) angle of 178.75(6)° is nearly ideal (Table 2), the Cl(1)−Ru−Cl(2) vector is tilted away by ca. 8° from the normal to the RuP_4 plane along the P(1)−P(3) vector. Both chelate rings have an envelope conforma-

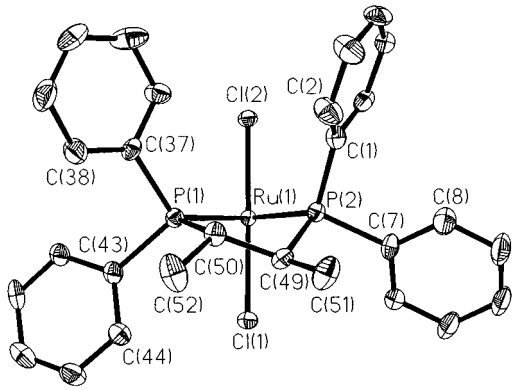

Figure 4. ORTEP view of $[RuCl_2(chiraphos)_2]$ (**2b**) along the RuP_4 plane. The second chiraphos ligand is omitted for clarity.

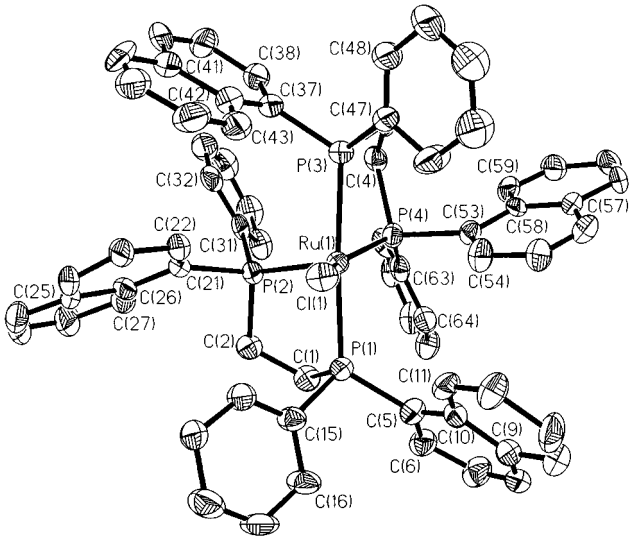

Figure 5. ORTEP view of $[RuCl(bnpe)_2][PF_2O_2]$, **3a**.

tion with the four methyl groups in pseudo-equatorial positions. The two flaps are on P(2) and P(3), which are displaced on opposite sides of the RuP_4 plane. In the first chelate, Ru, P(1), C(49), and C(50) are coplanar within ±0.11 Å, and P(2) is displaced from their mean plane by 0.85 Å (Figure 4). In the second one, Ru, P(4), C(53), and C(54) are coplanar within ±0.09 Å, and P(3) is displaced by 0.82 Å. This results in an proximate *syn*-diaxial,*syn*-diequatorial conformation for the four phenyls in both chiraphos ligands. Thus, despite the stereocenters on the diphosphine backbone, the molecule is nearly centrosymmetric, and the phenyl groups are arranged with a pseudo-C_{2h} symmetry (2/*m*). Finally, the axial phenyl groups on P(1) and P(3) point toward the Cl atoms and open the corresponding Cl−Ru−P angles to about 98°, as indicated by the short Cl···C contacts (Table 2). As observed for **2a**, the Ru−Cl and Ru−P distances are long due to steric crowding.[18]

$[RuCl(bnpe)_2]PF_6$. The reaction of **2a** with $Tl[PF_6]$ in CH_2Cl_2 gives the five-coordinate, cationic complex $[RuCl(bnpe)_2]PF_6$ (**3a**), as confirmed by an X-ray study (Figure 5, Table 3). The unit cell contains two crystallographically independent $[RuCl(bnpe)_2]^+$ cations, one $[PF_2O_2]^-$ anion, one (μ-H)-bridged $[PF_2O_2H\cdots O_2F_2P]^-$ unit, one (μ-H)$_2$-bridged $[PF_2O_2H]_2$ dimer, and two CH_2Cl_2 molecules. The presence of the $[PF_2O_2]^-$ anion, possibly formed by hydrolysis of $[PF_6]^-$,[21] is confirmed

Table 3. Selected Interatomic Distances (Å) and Angles (deg) in $[RuCl(bnpe)_2]PF_2O_2$ (2b)

Ru(1)−Cl(1)	2.400(4)		
Ru(1)−P(1)	2.391(4)	Ru(1)−P(2)	2.283(4)
Ru(1)−P(3)	2.468(4)	Ru(1)−P(4)	2.315(4)
Ru(1)···C(22)	3.61(1)	Ru(1)···C(54)	3.13(2)
Ru···H−C(22)	3.00	Ru···H−C(54)	2.40
Cl(1)−Ru(1)−P(1)	89.7(1)	Cl(1)−Ru(1)−P(2)	112.9(2)
Cl(1)−Ru(1)−P(3)	86.6(1)	Cl(1)−Ru(1)−P(4)	151.8(2)
P(1)−Ru(1)−P(2)	82.6(1)	P(1)−Ru(1)−P(3)	174.4(2)
P(1)−Ru(1)−P(4)	99.3(1)	P(2)−Ru(1)−P(3)	102.6(1)
P(2)−Ru(1)−P(4)	94.8(1)	P(3)−Ru(1)−P(4)	82.2(2)
Ru(1)−P(1)−C(5)	122.8(5)	Ru(1)−P(2)−C(21)	115.6(5)
Ru(1)−P(3)−C(37)	121.4(5)	Ru(1)−P(4)−C(53)	103.5(5)

by ^{31}P NMR. As the two cations are very similar, only one will be discussed here. As expected for a π-stabilized, 16-electron complex, $[RuCl(bnpe)_2]^+$ has a distorted trigonal bipyramidal geometry (Y-shaped).[22] Other typical features are the shorter Ru−Cl bond (2.400(4) Å) than in the 18-electron complex **2a** (2.449(1) and 2.457(1) Å) and the characteristically narrow P(2)−Ru−P(4) angle of 94.8(1)°. The conformation at ruthenium is Λ in both independent molecules. Each chelate ring has an envelope conformation, but, at difference with **2a**,**b**, the flap is located on a C atom.[23] However, the conformation of the substituents at the P atoms is virtually the same as observed in the six-coordinate **2a**, i.e., approximately *syn*-diaxial,*syn*-diequatorial.

The Y-shaped equatorial plane is distorted, with largely different Cl−Ru−P angles (112.9(2)° and 151.8(2)°), as already observed in analogous systems.[24−26] The latter feature is coupled with a short nonbonded contact of 3.13(2) Å between Ru and C(54). This is the C^2 atom of the naphthyl group approaching the metal on the sixth coordination site left open by the large Cl−Ru−P(1) angle.[27] The resulting calculated Ru···H−C contact (2.40 Å, $\Psi = 129.4°$) suggests a weak to medium γ-agostic interaction,[28] which stabilizes the electron-deficient complex together with steric effects,[29] as observed in other 16- or 14-electron complexes of ruthenium(II).[30] The Ru−P−C(naphthyl) angles suggest that there is an attractive interaction between Ru and C(54). The smallest Ru−P−C angle is the one involved in the agostic interaction, Ru(1)−P(4)−C(53) (103.5(5)°).

(21) Jeffery, J. C.; Jelliss, P. A.; Lebedev, V. N.; Stone, F. G. A. *Organometallics* **1996**, *15*, 4737.

(22) (a) Caulton, K. G. *New J. Chem.* **1994**, *18*, 25. (b) Riehl, J.-F.; Jean, Y.; Eisenstein, O.; Pélissier, M. *Organometallics* **1992**, *11*, 729. (c) Johnson, T. J.; Folting, K.; Streib, W. E.; Martin, J. D.; Huffman, J. C.; Jackson, S. A.; Eisenstein, O.; Caulton, K. G. *Inorg. Chem.* **1995**, *34*, 488, and references therein.

(23) In the first molecule, Ru, P(3), P(4), and C(3) are perfectly coplanar, with C(4) at 0.74 Å from their plane, whereas Ru, P(1), P(2), and C(2) are coplanar within ±0.09 Å, and C(1) is displaced by 0.70 Å from the mean plane.

(24) Mezzetti, A.; Del Zotto, A.; Rigo, P.; Bresciani Pahor, N. *J. Chem. Soc., Dalton Trans.* **1989**, 1045.

(25) Batista, A. A.; Centeno Cordeiro, L. A.; Oliva, G. *Inorg. Chim. Acta* **1993**, *203*, 185.

(26) Chin, B.; Lough, A. J.; Morris, R. H.; Schweitzer C. T.; D'Agostino, C. *Inorg. Chem.* **1994**, *33*, 6278.

(27) The next closest contact is Ru···C(22) (3.61(1) Å).

(28) (a) Brookhart, M.; Green, M. L. H.; Wong, L.-L. *Prog. Inorg. Chem.* **1988**, *36*, 1. (b) Crabtree, R. H.; Holt, E. M.; Lavin, M.; Morehouse, S. M. *Inorg. Chem.* **1985**, *24*, 1986. (c) Crabtree, R. H. *Angew. Chem., Int. Ed. Engl.* **1993**, *32*, 789. (d) Yao, W.; Eisenstein, O.; Crabtree, R. *Inorg. Chim. Acta* **1997**, *254*, 105.

(29) (a) Cooper, A. C.; Streib, W. E.; Eisenstein, O.; Caulton, K. G. *J. Am. Chem. Soc.* **1997**, *119*, 9069. (b) Ujaque, G.; Cooper, A. C.; Maseras, F.; Eisenstein, O.; Caulton, K. G. *J. Am. Chem. Soc.* **1998**, *120*, 361.

A low-temperature NMR investigation of **3a** in CD_2Cl_2 was directed to assess the agostic interaction in solution. The room-temperature ^{31}P NMR spectrum shows a static spectrum with two pseudo-triplets at δ 65.4 (P_{eq}) and 46.6 (P_{ax}). This indicates that one conformation of the chelate rings is preferred (the Λ one is observed in the solid state). Alternatively, the exchange between P_{ax} and P_{eq}, which switches the Δ and Λ configurations, must be slow on the NMR time scale. Also, there is fast exchange between C(54) and C(22), as the four P atoms are equivalent in pairs at room temperature. Broadening of the P_{eq} triplet occurs upon cooling below −50 °C, suggesting that this exchange process slows down. The signals of the H atoms at the 2-position of the equatorial naphthyl groups (C(54) and C(22) in the X-ray structure) were attributed by NOESY and P−H correlation 2D spectroscopy at −70°. However, they exchange rapidly with each other even at −70 °C. Thus, the corresponding $J_{C,H}$ value (158 Hz) has little significance, but disfavors a strong agostic interaction.

Finally, the conformational features of the diphosphines in **2a**,**b** and **3a** deserve a comment. Examining the CSD database, Seebach and co-workers have found that a number of complexes containing chiral bidentate phosphines exhibit pseudo-C_s-symmetry due to the flattened conformation of one of the PPh_2 groups,[31] similarly to our findings in **2a**,**b** and **3a**. They also discussed the relationship between the symmetry of the chelate ring and that of the conformation of the PPh_2 groups and proposed a distinction between C_2- and C_1-symmetric ligands. Chiraphos has been long considered a conformationally rigid ligand, with the chelate ring in a twist conformation that forces the PPh_2 groups in a C_2-symmetric "edge-on/face-on" conformation.[32] Also in disubstituted complexes, such as *cis*-[IrH_2((*S*,*S*)-chiraphos)$_2$]$^+$, both chiraphos ligands assume a twist (δ) conformation.[33] However, recent investigations have shown that the alternative envelope conformation also occurs, at least in the solid state, as in the π-allyl complex [Pd(η^3-PhCHCHCHPh)(chiraphos)]PF_6.[34] The flexibility of the chiraphos backbone is illustrated also by [Ru(L)(chiraphos)(C_5H_5)]$^+$. Changing the ligand L from (chiral) S(Me)(O)(Ph) to (achiral) SMe_2 switches the conformation of the phenyl rings from C_1- to C_2-symmetric.[35] Thus, rather than an intrinsic property of the ligand,[31,32] the conformation of the substituents at the P atoms in coordinated diphosphines appears to depend on the coordination environment as a whole. We suggest that the configuration and steric crowding of the complex play an important role and discuss the effects of this conformational flexibility of chiraphos on catalysis below.

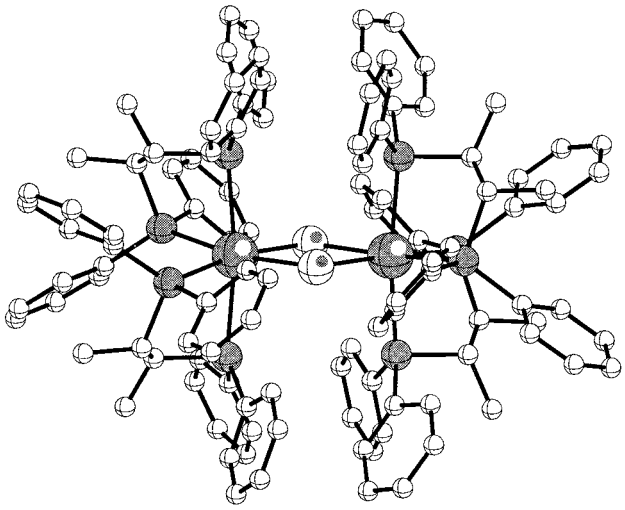

Figure 6. Ball-and-stick view of the D_2-symmetric dimer [Ru_2Cl_2(chiraphos)$_4$]$^{2+}$ (Cerius^2 molecular modeling calculations).

Chart 2

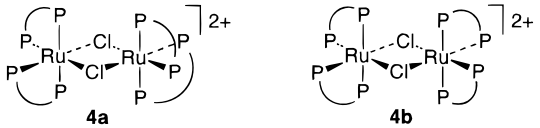

4a 796 kcal mol^{-1} **4b** 852 kcal mol^{-1}

[RuCl(chiraphos)$_2$]$_2$[PF_6]$_2$. Similarly to **2a**, [$RuCl_2$(chiraphos)$_2$] (**2b**) reacts with Tl[PF_6] in CH_2Cl_2 giving a product analyzing as [RuCl(chiraphos)$_2$]PF_6 (**3b**). However, the ^{31}P NMR spectrum in CD_2Cl_2 solution (in the concentration range 5−20 mM) shows signals that are better attributed to the dimers [(chiraphos)$_2$Ru(μ-Cl)$_2$(chiraphos)$_2$]$^{2+}$ (**4a**,**b**) rather than to five-coordinate **3b**. The major species present in solution (95% integrated intensity) shows two pseudo-triplets (AA′XX′, δ 51.9, 38.6, $J_{P,P'}$ = 22.6 Hz). A minor component (ca. 5%) exhibits two apparent AA′XX′ systems (δ 52.6, 47.1, $J_{P,P'}$ = 27.8 Hz; δ 40.8, 38.1, $J_{P,P'}$ = 21.4 Hz). The chemical shifts of both species are indicative of a six-coordinate structure rather than a five-coordinate one.[24,26] As two diastereomers are possible for the binuclear species [Ru_2Cl_2(chiraphos)$_4$]$^{2+}$, we suggest that the major signals are those of the D_2-symmetric isomer **4a**, whereas the low-intensity ones are those of the C_2-symmetric **4b** (Chart 2). Molecular modeling suggests that two five-coordinate fragments **3b** can form μ-dichloro-bridged dimers [(P−P*)$_2$Ru(μ-Cl)$_2$Ru(P−P*)$_2$]$^{2+}$ (**4a**,**b**) (P−P* = chiraphos). UFF calculations based on the Cerius^2 program[36] give energy values that are in qualitative agreement with the observed isomer distribution, with **4b** at higher energy than **4a** (Chart 2). The minimized structure of the D_2-symmetric dimer **4a** is shown in Figure 6.

Complexes **4a**,**b** partially dissociate to the five-coordinate cation [RuCl(chiraphos)$_2$]$^+$ in $CDCl_3$ solution

(30) For recent examples, see: (a) Martelletti, A.; Gramlich, V.; Zürcher, F.; Mezzetti, A. *New J. Chem.* **1999**, 199. (b) Baratta, W.; Herdtweck, E.; Rigo, P. *Angew. Chem.* **1999**, *111*, 1733. (c) Huang, D.; Huffman, J. C.; Bollinger, J. C.; Eisenstein, O.; Caulton, K. G. *J. Am. Chem. Soc.* **1997**, *119*, 7398. (d) Huang, D.; Streib, W. E.; Eisenstein, O.; Caulton, K. G. *Angew. Chem., Int. Ed. Engl.* **1997**, *36*, 2004. (e) Ogasawara, M.; Saburi, M. *Organometallics* **1994**, *13*, 1911.

(31) Seebach, D.; Devaquet, E.; Ernst, A.; Hayakawa, M.; Kühnle, F. N. M.; Schweizer, W. B.; Weber, B. *Helv. Chim. Acta* **1995**, *78*, 1636.

(32) (a) Orpen, A. G. *Chem. Soc. Rev.* **1993**, *22*, 191. (b) Halpern, *J. Science* **1982**, *217*, 401. (c) Of notice, (*R*,*S*)-2,3-bis(diphenylphosphino)-butane mantains the C_2-conformation in [RhCl((*R*)-P(Men)Ph_2)((*R*,*S*)-chiraphos)]: Gugger, P.; Limmer, S. O.; Watson, A. A.; Willis, A. C.; Wild, S. B. *Inorg. Chem.* **1993**, *32*, 5692.

(33) Brown, J. M.; Evans, P. L.; Maddox, P. J.; Sutton, K. H. *J. Organomet. Chem.* **1989**, *359*, 115.

(34) Yamaguchi, M.; Yabuki, M.; Yamagishi, T.; Kondo, M.; Kitagawa, S. *J. Organomet. Chem.* **1997**, *538*, 199.

(35) Schenk, W. A.; Frisch, J.; Dürr, M.; Burzlaff, N.; Stalke, D.; Fleischer, R.; Adam, W.; Prechtl, F.; Smerz, A. K. *Inorg. Chem.* **1997**, *36*, 2372.

(36) (a) Rappé, A. K.; Casewit, C. J.; Colwell, K. S.; Goddard, W. A., III; Skiff, W. M. *J. Am. Chem. Soc.* **1992**, *114*, 10024. (b) Rappé, A. K.; Colwell, K. S.; Casewit, C. J. *Inorg. Chem.* **1993**, *32*, 3438.

(eq 1). The ^{31}P NMR spectrum in $CDCl_3$ (8×10^{-3} mol

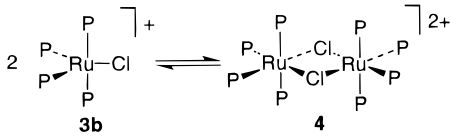

(1)

L^{-1}) shows two broad triplets at δ 63.2 and 58.6 ($J_{P,P'} \cong 25$ Hz), downfield of the signals of dimers **4a**,**b**. The chemical shifts of the former are similar to those of **4a** and other $[RuCl(P-P)_2]^+$ complexes with diphosphines forming five-membered rings.[24,26] Integration of the spectrum indicates that 47% of the complex is present as the monomer $[RuCl(chiraphos)_2]^+$ at room temperature and the remaining part as dimer **4**. Upon raising the temperature to 50 °C, the equilibrium shifts toward the monomer (68%), whose signals coalesce in a broad hump at δ 62, as expected for a fluxional five-coordinate complex. The occurrence of equilibrium 1 is further supported by spectrophotometric measurements. The electronic spectrum of **4** in 4.5×10^{-3} mol L^{-1} $CHCl_3$ solution shows the features of six-coordinate ruthenium(II) complexes, with a shoulder at 350 nm and a band at 450 nm ($\epsilon = 380$ L mol^{-1} cm^{-1}). However, the extinction coefficient ϵ of the latter band increases as the concentration is lowered ($\epsilon = 720$ mol^{-1} cm^{-1} at $C = 1.8 \times 10^{-4}$ mol L^{-1}), and two shoulders appear at 555 and 630 nm, in the region observed for five-coordinate **3a**. This suggests that the solution contains a five-coordinate complex,[12,24] whose concentration increases by lowering the concentration. The different tendency of **3a** and **3b** toward dimerization can be rationalized in terms of the larger steric bulk of bnpe as compared to chiraphos.

Reactivity of $[RuCl(P-P)_2]^+$. The five-coordinate species **3a**,**b** react with carbon monoxide to give the carbonyl complexes *trans*-$[RuCl(CO)(P-P^*)_2]^+$. In line with the presence of five-coordinate $[RuCl(chiraphos)_2]^+$ in $CDCl_3$ solution, **3b** reacts instantaneously with CO in $CDCl_3$ to give $[RuCl(CO)(chiraphos)_2]^+$ (**5b**). This also indicates that equilibrium 1 is rapidly established. The bnpe analogue **3a** reacts reluctantly. No reaction is observed between **3a** and CO at room temperature in $CDCl_3$ during 24 h. The carbonyl derivative *trans*-$[RuCl(CO)(bnpe)_2]^+$ (**5a**) is formed by reacting **3a** with CO at 50 °C in $CDCl_3$ for 12 h. As 16-electron complexes usually react very rapidly with CO, this unusual behavior is further evidence that the sixth coordination position of **3a** is shielded by a naphthyl group, as observed in the solid state. Accordingly, the relatively crowded five-coordinate species $[RuCl(dppp)_2]^+$ does not react with CO at temperatures lower than −40 °C.[37]

Asymmetric Cyclopropanation. Recently, ruthenium-catalyzed cyclopropanation has attracted growing interest.[2] Although catalytic systems based on N- and P,N-donor ligands have been reported,[7b,8] the application of bis(diphosphine) complexes is new.[38] Unsaturated cationic ruthenium complexes are expected to be more reactive than neutral ones.[8a] Thus, we tested **3a**,**b** as catalyst precursors in the asymmetric cyclopropanation of styrene. For comparison's sake, the achiral $[RuCl(dppp)_2]PF_6$ (**3c**)[12] was also tested. The complexes **3a**−**c** (1 mol %) catalyze the cyclopropanation of styrene by ethyl diazoacetate to give the corresponding 2-phenylcyclopropane carboxylates (Scheme 2). All catalysts give both *E*- and *Z*-isomers with approximately the same ratio (ca. 55:45, Table 4), which lies in the range of diastereoselectivity generally obtained with ethyl diazoacetate.[39] The reaction is highly chemoselective, as neither dimerization (fumarate and maleate) nor homologation products are observed with **3a**−**c**. The ^1H NMR spectrum of the reaction mixture shows unreacted diazoacetate after the reaction has stopped (6 h reaction time). The conversions obtained (∼40% based on the diazoacetate) are similar to those obtained with other phosphino complexes of ruthenium.[38]

Scheme 2

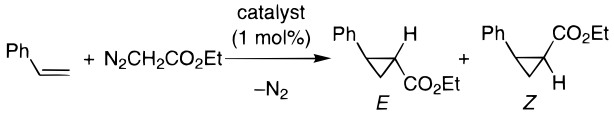

Table 4. Catalytic Cyclopropanation of Styrene[a]

					selectivity (ee) (%)	
run	cat.	*T* (°C)	*t* (h)	conv. (%)	*E*	*Z*
1	**3b**	20	1	37	54 (25)	46 (6)
	3b	20	6	55	56 (14)	44 (16)
2[b]	**3b**	20	6	38	56 (10)	44 (35)
3	**3b**	0	1	29	58 (25)	42 (14)
	3b	0	6	40	56 (21)	44 (7)
4	**3a**	20	1	24	54 (5)	46 (6)
	3a	20	6	37	55 (<5)	45 (11)
5[b]	**3c**	20	6	38	56 (−)	44 (−)

[a] Reaction conditions: ethyl diazoacetate (1 mmol) in CH_2Cl_2 (1 mL) was added dropwise to a CH_2Cl_2 solution (5 mL) of styrene (20 mmol), the catalyst (0.01 mmol), and decane (1 mmol) as internal GC standard. [b] In 20 mL of CH_2Cl_2.

The chiraphos derivative **3b** induces moderate enantioselectivity, giving up to 35% ee for the *Z*-product (run 2) and to 25% for the *E*-isomer (run 1, after 1 h). Monitoring by chiral GC shows that the ee values of both diastereomers are not constant throughout the reaction. With **3b**, the enantiomeric excess of the *E*-product drops from 25% after 1 h to 14% after 6 h reaction time, whereas that of the *Z*-product increases from nearly racemic to 16% (run 1). As most of the substrate is converted within 1 h, we suspect that the enantioselectivity drops due to catalyst degradation.[40] Lowering the temperature does not change either activity or selectivity (run 3). The bnpe derivative **3a** gives racemic products (run 4). As only few ruthenium carbene complexes have been isolated,[4f,1] some effort was spent attempting to trap the putative carbene intermediate $[RuCl(CH_2COOEt)(chiraphos)_2]^+$. The reaction of ethyl diazoacetate with **3b** gave an unstable complex

(37) Mezzetti, A.; Rigo, P. Unpublished results.

(38) For selected papers on ruthenium catalysts with monodentate phosphines, see: Demonceau, A.; Simal, F.; Jan, D.; Noels, A. F. *Tetrahedron Lett.* **1999**, *40*, 1653, and references therein.

(39) (a) The cis−trans ratio is usually increased with increasing bulkiness of the ester group of the diazoacetates within a row: Me < Et < *t*-Bu ≅ Men, according to diastereotopic face discrimination during the approach of the olefin on the Ru−carbene intermediate.[39b] (b) Nishiyama, H.; Itoh, Y.; Matsumoto, H.; Park, S.-B.; Itoh, K. *J. Am. Chem. Soc.* **1994**, *116*, 2223.

(40) However, the use of 5 mol % of the catalyst did not improve either conversion or ee.

(41) See, for instance: (a) Galardon, E.; Le Maux, P.; Toupet, L.; Simmoneaux, G. *Organometallics* **1998**, *17*, 565. (b) Nishiyama, H.; Aoki, K.; Itoh, H.; Iwamura, T.; Sakata, N.; Kurihara, O.; Motoyama, Y. *Chem. Lett.* **1996**, 1071.

Chart 3

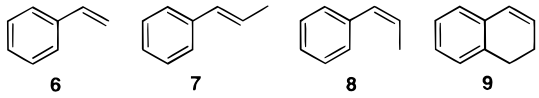

Scheme 3

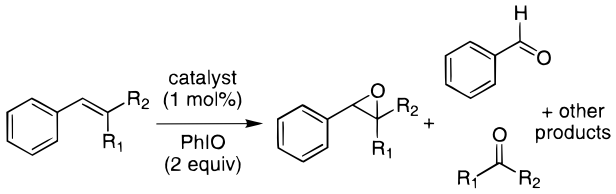

that decomposed in solution within 3 h, giving the fumarate and maleate esters, as detected by GC analysis. The low stability of this species precluded ^{13}C NMR and MS studies.

We suggest two explanations for the low (or lack of) asymmetric induction observed with **3a**,**b**. First, inefficient enantioface selection can result from a six-coordinate carbene intermediate[8a,c] having a pseudo-C_s-symmety similar to that observed in **2a**,**b**.[2,39b] An analogous explanation holds also for [RuCl$_2$(P)$_3$] (P$_3$ = chiral triphosphine).[8a] Second, as we observe a significant blank reaction in the absence of the catalyst (ca. 20% conversion), the low enantioselectivity might be explained by a concurrent, non-metal-catalyzed pathway. In conclusion, the systems based on P$_4$ (and P$_3$ donor sets)[8a,b] are less efficient that those based on N$_4$ and P$_2$N$_2$ donors.[7b,8c] Improved ligand design and enhancement of the catalytic activity are clearly required.

Asymmetric Epoxidation. Complexes **3a**,**b** were tested as catalyst precursors in the epoxidation of unfunctionalized alkenes with iodosyl benzene (PhIO) as primary oxidant. Styrene (**6**), *trans*-*β*-methylstyrene (**7**), *cis*-*β*-methylstyrene (**8**), and 1,2-dihydronaphthalene (**9**) were chosen as model substrates (Chart 3). The overall reaction is shown in Scheme 3. The main products are the epoxide, PhCHO (and other aldehydes) from the oxidative cleavage of the C=C bond, and the polymer of the olefin. In general, good to excellent olefin conversions are achieved with all substrates, but neither the bnpe nor the chiraphos complexes **3a**,**b** give any chiral induction. The reaction conditions were optimized using [RuCl(dppp)$_2$]PF$_6$ (**3c**) as catalyst precursor on the lines of Bressan's work.[11] We found that adding the primary oxidant PhIO in batches dramatically increases both the olefin conversion (60−100%) and the selectivity for the epoxide (up to 51%) (Table 5). In the optimized catalytic run, solid PhIO was added in portions (13 × 0.15 mmol) to a CH$_2$Cl$_2$ solution of the olefin (1.0 mmol) and catalyst (10 μmol, 1 mol %) under argon over a time of 6 h. The course of the reaction was monitored by GC for 7 h. Control experiments show that the epoxidation proceeds only in the presence of both the oxidant and the catalyst.

In contrast with what is generally observed with ruthenium-based catalysts,[42] epoxidation effectively competes with oxidative cleavage (Table 5). Thus, **3a** and **3c** yield styrene oxide with 30−35% selectivity (runs 1, 3), whereas the bnpe derivative **3a** gives mainly

Table 5. Catalytic Epoxidation[a]

				selectivity (%)	
run	cat.	olefin	conv. (%)	epoxide	PhCHO
1	**3a**	**6**	100	35	24
2	**3b**	**6**	74	3	33
3	**3c**	**6**	93	30	30
4	**3a**	**7**	64	51	38
5	**3b**	**7**	74	3	33
6	**3c**	**7**	92	41	35
7	**3a**	**8**	76	13[b]	<1
8	**3b**	**8**	84	33[c]	<1
9	**3c**	**8**	87	27[d]	<1
10	**3a**	**9**	100	4	
11	**3b**	**9**	100	2	
12	**3c**	**9**	97	42	

[a] Reaction conditions: PhIO (440 mg, 2.0 mmol) was added batchwise to a CH$_2$Cl$_2$ solution (5 mL) of the olefin (1.0 mmol), the catalyst (0.01 mmol), and decane as internal GC standard. Chiral GC analysis showed that racemic products are invariably formed with **3a**,**b**. [b] 4% of trans isomer is formed (based on converted olefin). [c] 0.3% of trans isomer is formed. [d] 3% of trans isomer is formed.

benzaldehyde (and formaldehyde, detected by ^{1}H NMR spectroscopy) (run 2). The missing mass in runs 1−3 is attributed to the formation of polystyrene, which was isolated according to the mass balance by addition of CH$_3$OH to the reaction solution, and identified by ^{1}H NMR spectroscopy. Similarly, the chiraphos and dppp complexes **3a** and **3c** epoxidize *trans*-*β*-methylstyrene (**7**) with high chemoselectivity (runs 4, 6). In the epoxidation of *cis*-*β*-methylstyrene (**8**), **3b** and **3c** give the best chemoselectivity (runs 7−9). As oxidative cleavage is negligible with all three catalysts, the missing mass is attributed to polymer formation. Interestingly, the reactions catalyzed by **3a**−**c** are stereospecific to a large extent: the major epoxidation product is *cis*-*β*-methylstyrene oxide (13−33% of the converted olefin), and *trans*-*β*-methylstyrene oxide is formed in minor amounts (0.3−4% of the converted olefin). This supports a concerted oxene transfer to the olefin, whereas Mn-based catalysts generally give a large amount of the *trans*-epoxide due to stepwise C−O bond formation.[3a,b,43] Finally, 1,2-dihydronaphthalene (**9**) gives quantitative conversion, but the epoxide is not stable under the reaction conditions (runs 10−12). GC monitoring showed that, as the reaction proceeds, the epoxide is converted to other products that were not identified.

The catalytic reaction was monitored by ^{31}P and ^{1}H NMR spectroscopy in order to determine the fate of the catalyst. Solid PhIO (0.68 equiv vs styrene) was added to a CD$_2$Cl$_2$ solution containing styrene and **3a** (50:1 mol ratio). The formation of styrene oxide, PhCHO, and HCHO was observed by ^{1}H NMR. After ca. 2 h, catalytic activity ceases due to oxidant consumption, and the ^{31}P{^{1}H} NMR spectrum shows the Ru complex and bnpe oxide (29% of starting **3a**). Catalytic activity resumes after addition of PhIO, and quantitative substrate conversion is achieved. NMR spectroscopic analyses ∼2 h after each addition of oxidant reveal further decomposition of the Ru complex to give bnpe dioxide, but ca. 16% of starting **3a** is present after complete substrate conversion, showing that the catalyst survives (at least in part) during the reaction. On the basis of this

(42) Barf, G. A.; Sheldon, R. A. *J. Mol. Catal. A-Chem.* **1995**, *102*, 23.

(43) Chang, S.; Galvin, J. M.; Jacobsen, E. N. *J. Am. Chem. Soc.* **1994**, *116*, 6937.

observation, and precedents of asymmetric epoxidation of terminal olefins catalyzed by platinum complexes containing chiral diphosphines,[44] we suspect that the lack of chiral induction with **3a**,**b** is due to the pseudo-C_s-symmetry in the oxo intermediate $[RuCl(O)(P-P^*)_2]^+$. The latter species is the putative oxene-transfer reagent based on previous mechanistic studies[11a] and on the isolation of the osmium analogue *trans*-$[OsCl(O)(dcpe)_2]^+$ (dcpe = 1,2-bis(dicyclohexylphosphino)ethane).[45,46] However, as partial oxidative degradation of the P−P* ligand occurs, the lack of asymmetric induction could also be due to the formation of an achiral complex.

Conclusion. In the bis(diphosphino) complexes $[RuCl_n(P-P^*)_2]^{(2-n)+}$ ($n = 1, 2$; P−P* = chiraphos or bnpe), the aryl substituents at the P atoms assume a pseudo-C_s-symmetric conformation due to the envelope conformation of the five-membered chelate ring. This is apparently independent of whether the stereogenic centers are C or P atoms and of the nature of the aryl group (either phenyl or 1-naphthyl). Our results confirm that chiraphos can assume different conformations, depending on the coordination environment. The results of the catalytic reactions reported herein, the first ones using chiral bis(diphosphino) complexes of the type $[RuCl(P-P^*)_2]^+$, suggest that a pseudo-C_s-symmetric conformation of the diphosphine correlates with low enantioselectivity also in reactions occurring at an octahedral complex without precoordination of the substrate. We are addressing this problem with an improved design of the ligands $R^1R^2P-PR^1R^2$ using R^1 and R^2 substituents having largely different steric bulks, and studying other catalytic applications of the $[RuX(P-P^*)_2]^+$ complexes.

Experimental Section

General Comments. Reactions with air- or moisture-sensitive materials were carried out under an argon atmosphere using standard Schlenk techniques. Olefins and solvents were purified according to standard procedures. Yields of complexes are based on ruthenium. ^1H, ^{31}P, and ^{13}C NMR spectra were measured on a Bruker DPX 250 spectrometer. ^1H (and ^{13}C) and ^{31}P positive chemical shifts in ppm are downfield from tetramethylsilane and external 85% H_3PO_4, respectively. The ^1H and ^{31}P NMR spectra of the P→BH_3 borane adducts P(BH$_3$)(Me)(Ph)(1-Np) and **1a**·(BH$_3$)$_2$ are partially relaxed, non-binomial 1:1:1:1 quartets due to coupling to ^{11}B (80.1% natural abundance). The $J_{B,H}$ and $J_{P,B}$ coupling constants were measured between the central peaks. Mass spectra were measured by the MS service of the Laboratorium für Organische Chemie (ETH Zürich) using a ZAB VSEQ mass spectrometer. A 3-NOBA (3-nitrobenzyl alcohol) matrix and a Xe atom beam with a translation energy of 8 keV were used for FAB^+ MS. Gas chromatographic analyses were performed using a Carlo Erba 6000 Vega Series gas chromatograph and a Fisons Instruments GC 8000 Series gas chromatograph, both equipped with an FID detector. Species identification was made by comparison with authentic samples. HPLC was performed on a Hewlett-Packard 1050 chromatograph equipped with a variable wavelength detector and Daicel Chiralcel OD-H or OB-H columns (0.46 cm × 25 cm). Optical rotations were measured using a Perkin-Elmer 341 polarimeter with a 1 dm cell. Elemental analyses were carried out by the Laboratory of Microelemental Analysis (ETH Zürich). $[RuCl_2(PPh_3)_3]$,[47] *trans*-*β*-methylstyrene oxide, iodosyl benzene, 1,2-dihydronaphthalene oxide, *cis*-*β*-Me-styrene, and *cis*-*β*-Me-styrene oxide were prepared according to published methods (see Supporting Information). (*S*)-P(1-Np)(Ph)(Me)(BH$_3$) was prepared as previously described.[13d]

(*S*,*S*)-[(BH$_3$)(Ph)(1-Np)PCH$_2$CH$_2$P(BH$_3$)(Ph)(1-Np)], (*S*,*S*)-1a·(BH$_3$)$_2$. A hexane solution (6.25 mL, 1.1 M) of *sec*-BuLi (6.87 mmol) was added dropwise to a THF solution (60 mL) of (*S*)-P(BH$_3$)(Me)(Ph)(1-Np) (1.5 g, 5.67 mmol) at −78 °C. After the solution was stirred for 2.5 h, a suspension of anhydrous $[Cu(O_2C(CH_3)_3)_2]$ (4.51 g, 17.0 mmol) in THF (100 mL), cooled to −78 °C, was added by cannula. The resulting solution was allowed to reach room temperature overnight. The reaction was quenched with 1 M HCl (10 mL). The organic layer was diluted with ethyl acetate, washed twice with 1 M HCl, and neutralized with 1 M NaOH. The organic phase was extracted, and the product was separated by chromatography (silica gel, toluene/hexane, 1:1) from unreacted (*S*)-P(BH$_3$)(Me)(Ph)(1-Np) (343 mg). The latter exhibits the same enantiomeric purity as before the reaction and can be recycled. Chiral HPLC: (*S*,*S*):(*S*,*R*):(*R*,*R*) = 99.5:0.4:0.1 (OD-H, hexane/PrⁱOH/AcOEt= 98:1.5:0.5, R_t(*R*,*R*)-**1a**·(BH$_3$)$_2$ = 25.80 min, R_t(*R*,*S*)-**1a**·(BH$_3$)$_2$ = 29.18 min, R_t(*S*,*S*)-**1a**·(BH$_3$)$_2$ = 32.64 min). Recrystallization from CH_2Cl_2/hexane (or AcOEt) gave **1a**·(BH$_3$)$_2$ as white microcrystals. Yield: 0.98 g (66%). Enantiomeric purity: >99%, only one enantiomer detected by HPLC. $[\alpha]^{20}_D = -32.1 \pm 0.12$ (C = 1, $CHCl_3$). ^1H NMR ($CDCl_3$) δ 7.95−7.09 (m, 24 H, arom), 2.60 (multiplet, 4 H, CH_2P). ^{31}P NMR ($CDCl_3$): 18.3 (br s, 2 P). MS (EI): *m*/*z* 511.2 ($M^+ - BH_4$, 5%), 498.2 ($M^+ - 2BH_3$, 59%), 362.1 ($M^+ - 2BH_3 -$ (Ph)PC_2H_4, 59%), 312.1 ($M^+ - 2BH_3 -$ (1-Np)PC_2H_4, 34%), 235.1 ($M^+ - 2BH_3 -$ (1-Np)(Ph)PC_2H_4, 41%) 233.1 ($M^+ - 2BH_3 -$ (1-Np)(Ph)$PC_2H_4 - 2H$, 100%). Anal. Calcd for $C_{34}H_{34}B_2P_2$·1/2AcOEt: C, 75.82; H, 6.72. Found: C, 75,75; H, 6.92.

(*S*,*S*)-[(Ph)(1-Np)PCH$_2$CH$_2$P(Ph)(1-Np)], (*S*,*S*)-1a. (*S*,*S*)-**1a**·(BH$_3$)$_2$ (0.52 g, 1 mmol) was dissolved in morpholine (30 mL), and the colorless solution was stirred overnight at room temperature. The yellowish solution was evaporated to dryness. Flash chromatography (alumina, toluene as eluent) yielded **1a** as a colorless oil. Yield: 0.46 g (94%). Enantiomeric purity: >99%, measured by reprotection with Me_2S·BH_3. The HPLC trace of resulting **1a** shows only one enantiomer under the above conditions. ^1H NMR ($CDCl_3$): δ 7.95−7.09 (m, 24 H, arom), 2.4−2.1 (m, 4 H, CH_2P). ^{31}P NMR ($CDCl_3$): −24.22 (*s*, 2 P). MS (EI): *m*/*z* 498.2 (M^+, 30%), 265.1 (M^+ − P(1-Np)(Ph) + 2H, 45%), 249.1 (M^+ − (Ph)(1-Np)PCH_2, 31%), 233.1 (M^+ − (Ph)(1-Np)PC_2H_4 − 2H, 91%), 149.1 (P(Ph)$(C_3H_5)^+$, 100%). Anal. Calcd for $C_{34}H_{28}P_2$·0.2CH_2Cl_2: C, 79.68; H, 5.86. Found: C, 79.86; H, 5.55.

(*l*)+(*u*)-[(BH$_3$)(Ph)(1-Np)PCH$_2$CH$_2$P(BH$_3$)(Ph)(1-Np)], (*l*)+(*u*)-1a·(BH$_3$)$_2$. The diastereomeric mixture was prepared as described for (*S*,*S*)-(bnpe)(BH$_3$)$_2$, but starting from (*rac*)-P(BH$_3$)(Me)(Ph)(1-Np) (210 mg). Yield: 138 mg (66%). ^1H NMR ($CDCl_3$): (*u*)-isomer (50%): 2.76 (br, 2 H, PC*HH*′), 2.42 (br, 2 H, PC*HH*′); (*l*)-isomer (50%): δ 2.60 (s, 4 H, PC*HH*′). ^{31}P NMR ($CDCl_3$): δ 18.31 (br, 2P, (*l*)- and (*u*)-isomers not resolved). Analytic and MS properties are as given for (*S*,*S*)-**1a**·(BH$_3$)$_2$.

***trans*-[RuCl$_2$(bnpe)$_2$], 2a.** $[RuCl_2(PPh_3)_3]$ (240 mg, 0.25 mol) and (*S*,*S*)-bnpe (250 mg, 0.5 mmol, 2 equiv) were placed in a Schlenk tube, and CH_2Cl_2 (5 mL) was added. The resulting solution was then stirred at room temperature for 6 h before it was reduced in volume to ∼1 mL. Upon addition of diethyl ether (10 mL) and partial evaporation of the solvents, a light brown precipitate was formed, which was filtered off, washed

(44) Sinigalia, R.; Michelin, R. A.; Pinna, F.; Strukul, G. *Organometallics* **1987**, *6*, 728.

(45) Barthazy, P.; Wörle, M.; Mezzetti, A. *J. Am. Chem. Soc.* **1999**, *121*, 480.

(46) However, metal−PhIO adducts have been suggested to react with olefins without the intermediacy of a metal−oxo species: Yang, Y.; Diederich, F.; Valentine, J. S. *J. Am. Chem. Soc.* **1991**, *113*, 7195.

(47) Hallman, P. S.; Stephenson, T. A.; Wilkinson, G. *Inorg. Synth.* **1970**, *12*, 237.

with hexane, and dried in a vacuum. Yield: 203 mg (69%). ^{1}H NMR ($CDCl_3$): δ 8.5−6.5 m (48 H, Ph and 1-Np), 3.12 d (br) (4 H, PC*HH*′), 2.53 d (br) (4 H, PC*HH*′). ^{31}P{^{1}H} NMR ($CDCl_3$): δ 38.4 (s). MS (FAB$^+$): *m*/*z* 1168.2 (M$^+$, 12%), 1133.2 (M$^+$ − Cl + H, 68%), 1097.2 (M$^+$ − 2Cl − H, 100%), 861.2 (M$^+$ − P(1-Np)(Ph)H, 25%), 634.0 (M$^+$ − Cl + H − bnpe, 40%), 599.1 (M$^+$ − 2Cl + H − bnpe, 74%). Crystals contain one mole of H_2O per mole of complex, as confirmed by ^{1}H NMR. Anal. Calcd for $C_{68}H_{56}Cl_2P_4Ru\cdot H_2O$: C, 68.80; H, 4.92. Found: C, 68.86; H, 4.83.

X-ray of [RuCl$_2$(bnpe)$_2$], 2a. Crystals of **2a** were obtained by diffusion of hexane into a $CDCl_3$ solution of **2a** at room temperature. Crystal data: $C_{58}H_{56}Cl_2P_4Ru$ orange platelet, *M* =1168.98, *T* = 293 K, orthorhombic, $P2_12_12_1$, *a* = 11.5658(4) Å, *b* = 22.6250(9) Å, *c* = 22.8667(9) Å, *V* = 5983.7(4) Å^3, *F*(000) = 2408, *Z* = 4, D_c = 1.298 Mg m^{-3}, μ(Mo Kα) = 0.498 mm^{-1}, crystal size 0.70 × 0.60 × 0.32 mm^3, Siemens SMART platform with CCD detector, normal focus molybdenum-target X-ray tube, graphite monochromator, ω-scans, *h*, −14 to 14, *k*, 0 to 28, *l*, 0 to 28; 37 098 reflections for 1.27° < θ < 26.37° (12 239 unique). Unit cell dimensions determination and data reduction were performed by standard procedures, and an empirical absorption correction (SADABS) was applied. The structure was solved with SHELXS-96 using direct methods and refined by full-matrix least-squares on F^2 with anisotropic displacement parameters for all non-H atoms. Hydrogen atoms were introduced at calculated positions on nondisordered C atoms of the cation and refined with the riding model and individual isotropic thermal parameters. R1 = 0.0468 and wR2 = 0.1363 (9871 unique reflections with $I > 2\sigma(I)$), R1 = 0.0671, and wR2 = 0.1498 (all data), GOF = 1.162. Max. and min. difference peaks 1.189 and −0.398 e Å^{-3}, largest and mean Δ/σ were 0.230 and 0.007. Selected bond lengths and angles are given in Table 1.

[RuCl$_2$(chiraphos)$_2$], 2b. [RuCl$_2$(PPh$_3$)$_3$] (224 mg, 0.23 mmol) and (*S*,*S*)-chiraphos (200 mg, 0.45 mmol) were dissolved in CH_2Cl_2 (5 mL). After stirring the red-brown solution for 4 h, hexane (10 mL) was added, and CH_2Cl_2 was evaporated in a vacuum. The resulting light yellow precipitate was filtered off, washed with hexane, and dried in a vacuum. ^{1}H NMR spectroscopy shows that the solid contains 1 mol CH_2Cl_2 per mole of complex. Yield: 230 mg (90%). ^{1}H NMR ($CDCl_3$): 7.8−6.7 (m, 40 H, arom), 2.9−2.7 (br m, 4 H, PC*H*), 0.65 (br m, 12 H, C*H*$_3$). ^{31}P{^{1}H} NMR ($CDCl_3$): δ 47.0 (s, 4P). Anal. Calcd for $C_{56}H_{56}Cl_2P_4Ru\cdot CH_2Cl_2$: C, 61.69; H, 5.27. Found: C, 61.42; H, 5.35.

X-ray of [RuCl$_2$(chiraphos)$_2$], 2b. Crystals of **2b** were obtained by diffusion of Et_2O into a $CDCl_3$ solution of **2b**. Crystal data: $C_{112}H_{112}Cl_4P_8Ru_2$, orange platelet, *M* = 2049.72, *T* = 293 K, monoclinic, $P2_1$, *a* = 13.3497(5) Å, *b* = 17.9236(7) Å, *c* = 20.3450(7) Å, *V* = 4 858.9(3) Å^3, *F*(000) = 2120, *Z* = 4, D_c = 1.401 Mg m^{-3}, μ(Mo Kα) = 0.602 mm^{-1}, crystal size 0.64 × 0.28 × 0.22 mm^3, Siemens SMART platform with CCD detector, normal focus molybdenum-target X-ray tube, graphite monochromator, ω-scans, *h*, −17 to 16, *k*, −24 to 22, *l*, −25 to 26; 35 285 reflections for 1.00° < θ < 29.98° (20 542 unique). Data reduction and structure solution and refinement were as described above for **2a**. R1 = 0.0388 and wR2 = 0.0688 (11 643 unique reflections with $I > 2\sigma(I)$), R1 = 0.0989, and wR2 = 0.0848 (all data), GOF = 0.921 Max. and min. difference peaks 0.584 and −0.571 e Å^{-3}, largest and mean Δ/σ were 0.184 and 0.008. Selected bond lengths and angles are given in Table 2.

[RuCl(bnpe)$_2$]PF$_6$, 3a. *trans*-[RuCl$_2$(bnpe)$_2$] (**2a**) (200 mg, 0.17 mol) and Tl[PF_6] (110 mg, 0.192 mmol) were stirred in CH_2Cl_2 (5 mL) for 12 h. The resulting dark brown solution was filtered to remove the white precipitate TlCl, and to the filtrate was added Et_2O (10 mL). Evaporation of the solvents in a vacuum gave a brown solid, which was subsequently dried in a vacuum. Yield: 170 mg (88%). ^{1}H NMR (CD_2Cl_2, 20 °C): δ 9.17 (d, 2 H, arom), 8.4−6.5 (m, 44 H, arom), 5.90 (t, 2 H, equatorial Ph, *p*-C*H*), 2.6−2.2 (br m, 6 H, PC*HH*′); −70 °C: δ 9.17 (d, 2 H, Np−C*H*, $J_{H,H}$ = 8.6 Hz), 7.37 (br, 2 H, equatorial Ph, C^8*H*), 7.3−6.6 (m, 40 H, arom), 6.30 (br, 2 H, equatorial Np, C^2*H*), 5.90 (t, 2 H, equatorial Ph, *p*-C*H*), 2.6−2.2 (br m, 6 H, C*HH*′), 2.0−1.7 (br m, 2 H, C*HH*′). ^{31}P{^{1}H} NMR (CD_2Cl_2): δ 65.37 (t, AA′ part of AA′XX′, 2P, $J_{P,P'}$ = 17.5 Hz), 46.6 (t, XX′ part of AA′XX′, 2P, $J_{P,P'}$ = 17.5 Hz), δ −144.6 (septet, PF_6, $J_{P,F}$ = 713 Hz). UV−visible (CH_2Cl_2), λ (nm) (ϵ_{max} (mol^{-1} cm^{-1})): 350 (sh), 450 (1920), 555 (910), 630 (sh). MS (FAB$^+$): *m*/*z* 1133.2 (M$^+$, 91%), 1097.2 (M$^+$ − Cl − H, 100%), 599.1 (M$^+$ − 2Cl − H − bnpe, 16%). Anal. Calcd for $C_{68}H_{56}ClF_6P_5Ru\cdot H_2O$: C, 62.99; H, 4.51. Found: C, 63.13; H, 4.46.

X-ray of [RuCl(bnpe)$_2$][PF$_2$O$_2$], 3a. Red crystals were obtained by diffusion of hexane into a $CDCl_3$ solution of **3a**. Crystal data: $C_{138}H_{119}Cl_6F_{10}O_{10}P_{13}Ru_2$, red platelet, *M* = 2944.78, *T* = 293 K, tetragonal, $P4_1$, *a* = 17.3249(5) Å, *b* = 17.3249(5) Å, *c* = 45.528(2) Å, *V* = 13665.4(8) Å^3, *F*(000) = 6008, *Z* = 4, D_c = 1.431 Mg m^{-3}, μ(Mo Kα) = 0.561 mm^{-1}, crystal size 0.38 × 0.20 × 0.04 mm^3, Siemens SMART platform with CCD detector, normal focus molybdenum-target X-ray tube, graphite monochromator, ω-scans, *h*, −11 to 12, *k*, 0 to 17, *l*, −45 to 34; 11 094 reflections for 2.53° < θ < 20.81° (11 094 unique). Data reduction and structure solution and refinement were as described above for **2a**. R1 = 0.0764 and wR2 = 0.1826 (8788 unique reflections with $I > 2\sigma(I)$), R1 = 0.0991 and wR2 = 0.1970 (all data), GOF = 1.094. Max. and min. difference peaks 0.725 and −0.624 e Å^{-3}, largest and mean Δ/σ were 0.007 and 0.062. Selected bond lengths and angles are given in Table 2.

[RuCl(chiraphos)$_2$]PF$_6$, 3b. *trans*-[RuCl$_2$(chiraphos)$_2$] (**2b**) (130 g, 0.126 mmol) and Tl[PF_6] (82 mg, 0.192 mmol) were stirred in CH_2Cl_2 (5 mL) for 12 h. The resulting dark brown solution was filtered to remove TlCl, and hexane (10 mL) was added. Partial evaporation of the solvents yielded a brown solid, which was filtered off and dried in a vacuum. ^{1}H NMR spectroscopy shows that the solid contains CH_2Cl_2 (1 mol) and hexane (1 mol, per mole of complex). Yield: 103 mg (62%). ^{1}H NMR (CD_2Cl_2): D_2-symmetric dimer **4a** (95%), δ 7.8−6.7 (m, 80 H, aromatic), 3.2 (br m, 4 H, PC*H*), 2.5 (br m, 4 H, PC*H*′), 0.95−0.75 (br m, 24 H, C*H*$_3$). ^{31}P{^{1}H} NMR (CD_2Cl_2): D_2-symmetric dimer **4a** (95%), δ 51.9 (t, 2P, $J_{P,P'}$ = 22.6 Hz), 38.6 (t, 2P, $J_{P,P'}$ = 22.6 Hz); C_2-symmetric dimer **4b** (5%), δ 52.6 (t, 2P, $J_{P,P'}$ = 27.8 Hz), 47.1 (t, 2P, $J_{P,P'}$ = 27.8 Hz), 40.8 (t, 2P, $J_{P,P'}$ = 21.4 Hz), 38.1 (t, 2P, $J_{P,P'}$ = 21.4 Hz); −144.6 (septet, 1P, $J_{P,F}$ = 713 Hz, PF_6). ^{31}P{^{1}H} NMR ($CDCl_3$): monomer **3b** (47%): δ 63.2 (br, 2P), 58.6 (br, 2P); D_2-symmetric dimer **4a** (48%), δ 51.9 (t, 2P, $J_{P,P'}$ = 22.6 Hz), 38.6 (t, 2P, $J_{P,P'}$ = 22.6 Hz); C_2-symmetric dimer **4b** (5%), 52.6 (t, 2P, $J_{P,P'}$ = 27.8 Hz), 47.1 (t, 2P, $J_{P,P'}$ = 27.8 Hz), 40.8 (t, 2P, $J_{P,P'}$ = 21.4 Hz), 38.1 (t, 2P, $J_{P,P'}$ = 21.4 Hz); −144.6 (septet, 1P, $J_{P,F}$ = 713 Hz, PF_6). MS (FAB$^+$): *m*/*z* 1025.9 (M$^+$ + HCl, 6%), 989.0 (M$^+$, 54%), 952.9 (M$^+$ − HCl, 100%). MS (ESI, CH_2Cl_2): *m*/*z* 953.4 (M$^+$ − HCl, 100%). Anal. Calcd for $C_{56}H_{56}ClF_6P_5Ru\cdot C_6H_{14}\cdot CH_2Cl_2$: C, 57.96; H, 5.56. Found: C, 57.44; H, 5.35.

[RuCl(CO)(bnpe)$_2$]PF$_6$, 5a. A $CDCl_3$ solution of **3a** (23 mg, 18 μmol) was saturated with CO gas. The solution color turned from brown to pale yellow after 12 h at 50 °C. Evaporation of the solvent gave a pale yellow solid in quantitative yield. ^{1}H NMR ($CDCl_3$): δ 8.3−6.5 (m, 48 H, arom), 3.40 (br, 2 H, PC*HH*′), 3.03 (br, 2 H, PC*HH*′) 2.70 (br, 2 H, PC*HH*′), 2.02 (br, 2 H, PC*HH*). ^{31}P{^{1}H} NMR ($CDCl_3$): δ 48.08 (t, AA′ part of AA′XX′, 2P, $J_{P,P'}$ = 19.2 Hz), 32.1 (t, XX′ part of AA′XX′, 2P, $J_{P,P'}$ = 19.2 Hz), δ −144.6 (septet, PF_6, $J_{P,F}$ = 713 Hz). ^{13}C{^{1}H} NMR ($CDCl_3$): δ 201.3 (br, 1C, *C*O). MS (FAB$^+$): *m*/*z* 1161.1 (M$^+$, 100%), 1098.0 (M$^+$ − Cl − CO, 6%), 599.0 (M$^+$ − Cl − CO-bnpe, 64%).

[RuCl(CO)(chiraphos)$_2$]PF$_6$, 5b. A $CDCl_3$ solution of **3b** (22 mg, 19 μmol) was saturated with CO gas. The solution color turned instantaneously from brown to yellow. Evaporation of the solvent gave a pale yellow solid in quantitative yield. ^{1}H NMR ($CDCl_3$): δ 8.0−6.5 (m, 40 H, arom), 3.2 (br s, 2 H, PC*H*),

2.4 (br s, 2 H, PC*H*′), 0.8 (br m, 12 H, CH_3). $^{31}P\{^1H\}$ NMR ($CDCl_3$): δ 56.2 (t, AA′ part of AA′XX′, 2P, $J_{P,P'} = 22.4$ Hz), 34.4 (t, XX′ part of AA′XX′, 2P, $J_{P,P'} = 22.4$ Hz), δ −144.6 (septet, PF_6, $J_{P,F} = 713$ Hz). $^{13}C\{^1H\}$ NMR ($CDCl_3$): δ 199.8 (br, 1C, *C*O). MS (FAB^+): *m*/*z* 1017.2 (M^+, 100%), 953.2 ($M^+ - CO - H - Cl$, 65%), 591.0 (M^+ − chiraphos, 14%), 527.0 ($M^+ - CO - H - Cl$ − chiraphos, 34%).

Catalytic Cyclopropanation. A standard procedure was as follows. A CH_2Cl_2 solution (1 mL) of ethyl diazoacetate (114 mg, 1 mmol) was added dropwise over 4 h to a CH_2Cl_2 solution (5 mL) containing styrene (2.08 g, 20 mmol), the catalyst (0.01 mmol), and decane (1 mmol) as internal GC standard. The reaction solutions were kept under argon and at the desired temperature by means of a thermostatic bath. The evolution of N_2 gas was observed during the reaction. The reaction solutions were analyzed periodically by GC up to a total reaction time of 6 h. Achiral GC: fused silica capillary column (Macherey Nagel SE 54). Chiral GC: β-cyclodextrin capillary column (Supelco Beta Dex). Details of GC analyses are given in the Supporting Information. Results are reported in Table 4. Conversion is based on ethyl diazoacetate. The percent selectivity to product *a* is defined as (mol(*a*)/mol(converted diazoacetate)) × 100. The GC peak of *trans*-2-phenylcyclopropanecarboxylate ethyl ester was attributed by comparison with an authentic sample with a *E*/*Z* ratio of 99:1 (Lancaster). The latter was also used as authentic sample for chiral GC analysis. The absolute configuration of the cyclopropanation product was not determined.

Catalytic Epoxidation. A typical procedure was as follows. The olefin (freshly filtered over alumina, 1.0 mmol), decane (as internal GC standard, 35 mg), and **3a**−**c** (0.01 mmol, 1 mol %) were dissolved in CH_2Cl_2 (5 mL) under argon. After stirring the solution for 5 min, PhIO (440 mg, 2.0 mmol) was added in portions (13 × 34 mg) during 6 h. The reaction solution was analyzed over 7 h reaction time by GC. Achiral GC: fused silica capillary column (Supelco Optima δ-3). Chiral GC: α-cyclodextrin capillary column (Supelco Alpha Dex). Results are reported in Table 5. Olefin conversion is defined as the percentage of converted olefin, and the percent selectivity to product *a* is calculated as (mol(*a*)/mol(converted olefin)) × 100. The GC peaks of the enantiomeric epoxides were attributed by comparison with authentic samples of the racemates. Details of GC analyses are given in the Supporting Information. Monitoring of styrene epoxidation by NMR spectroscopy was as follows. A $CDCl_3$ solution (1 mL) containing **3a** (2 μmol) and styrene (100 μmol) was placed in an NMR tube under argon, and PhIO (15 mg, 68 μmol) was added thereto. The resulting slurry was shaken at room temperature, and the reaction was periodically checked by ^1H and ^{31}P NMR spectroscopy.

Acknowledgment. R.M.S. and T.Y.H.W. acknowledge the Swiss National Science Foundation for financial support.

Supporting Information Available: Tables of crystal data and structure refinement parameters, atomic coordinates, bond lengths and angles, anisotropic displacement parameters, and hydrogen coordinates of **2a**,**b** and **3a**, and details of catalytic reactions. This material is available free of charge via the Internet at http://pubs.acs.org.

OM990657X